Journal of Molecular Liquids 335 (2021) 116181

Contents lists available at ScienceDirect

Journal of Molecular Liquids

journal homepage: www.elsevier.com/locate/molliq

A first-principles evaluation on the interaction of 1,3,4-oxadiazole with pristine and B-, Al-, Ga-doped C_{60} fullerenes

İskender Muz [a,*], Mustafa Kurban [b,*]

[a] Department of Mathematics and Science Education, Nevşehir Haci Bektas Veli University, 50300, Nevşehir, Turkey
[b] Department of Electrical and Electronics Engineering, Kırşehir Ahi Evran University, 40100 Kırşehir, Turkey

ARTICLE INFO

Article history:
Received 13 February 2021
Revised 8 April 2021
Accepted 13 April 2021
Available online 17 April 2021

Keywords:
C_{60} fullerenes
1,3,4-oxadiazole
Surface interactions
Electronic sensitivity
DFT

ABSTRACT

In this study, the interaction of 1,3,4-oxadiazole with pristine and B-, Al-, Ga-doped C_{60} fullerenes were examined by density functional theory (DFT) for the first time. The results demonstrate that doping B, Al, Ga atoms on C_{60} enhance the chemical reactivity, however, reduces the electronic sensitivity toward the oxadiazole. Besides, doping B, Al, Ga atoms bring about a rise in the adsorption energy and energy gap. The highest adsorption capacity was calculated by doping Al, which is about −42.78 kcal.mol^{-1}. The WBI and FBO analyses indicate that possible bonding interactions with N or O atoms in the oxadiazole produce a considerable change in charge carrier mobility which in line with the map of electron density.

From the RDG analysis, the interaction between the oxadiazole and Al-doped C_{60} is in a strong interaction region, whereas B- and Ga-doped C_{60} are weak. The sensing capability of these systems tends to weaken by doping B, Al, Ga atoms.

1. Introduction

Recently, oxadiazoles and their derivatives have attracted intense scrutiny due to their various biological actions such as cytotoxic, antibacterial, antioxidant and anti-inflammatory [1–4]. More specifically, 1,3,4-oxadiazole and its derivatives, which is a thermally stable neutral aromatic molecule, has received substantial attention in the anti-diabetic, anti-malarial, antimicrobial, anticancer, analgesic, and anti-inflammatory [5–11].

Carbon-based materials (CBNs) such as fullerenes, graphene, and nanotubes have been used in many applications because of their excellent properties [12–23]. Among them, fullerenes, especially C_{60}, have been taken into consideration as a novel drug-delivery system and a sensor. Herein, many studies have been performed to detect different types of molecules using fullerene cages, but theoretical calculations have demonstrated that pure C_{60} is not much chemically reactive towards well-known gas molecules, owing to their weak interaction and poor charge transfer [17,24]. To overcome these difficulties, doping one or more atoms on CBNs has been performed to raise their surface reactivity and thus sensing efficiency [24–30]. For example, the adsorption capability of C_{60} for gas molecules improves by doping B, N, or Si [31–35]. The electronic properties C_{60} heterofullerenes are much sensitive for iodine detection by doping S atom [36]. Besides, an electron-deficient B-doped C_{60} gives rise to an enhancement in the adsorption energy of the O_2 molecule [37]. The electron-rich N doping can modulate the electronic structure of C_{60} [38–42].

Recently, oxadiazoles, especially 1,2,4 and 1,3,4 regioisomers, have emerged for their interesting biological properties as anticancer agents because they have high cytotoxicity towards malignant cells [43]. To reduce their cytotoxic effects on healthy cells and thus provide better anticancer efficacy, drug delivery tools, which are biocompatible and biodegradable, are used to deliver molecules in their active sites [25]. In this context, we carry out a first-principles evaluation on the interaction of 1,3,4-oxadiazole with pristine and B-, Al-, Ga-doped C_{60} using density functional theory (DFT) calculations for the first time. To get insights into the interactions of the oxadiazole with pristine and B-, Al-, Ga-doped C_{60}, the binding energy, the orbital energies (HOMO, LUMO), HOMO-LUMO energy gap, the density of states (DOS), vertical ionization potential and vertical electron affinity, chemical hardness, electrophilicity index are reported. To better understanding the bonding nature, the RDG, WBI and FBO analysis were analyzed in detail.

* Corresponding authors.
E-mail addresses: iskendermuz@yahoo.com (İ. Muz), mkurbanphys@gmail.com (M. Kurban).

https://doi.org/10.1016/j.molliq.2021.116181
0167-7322/

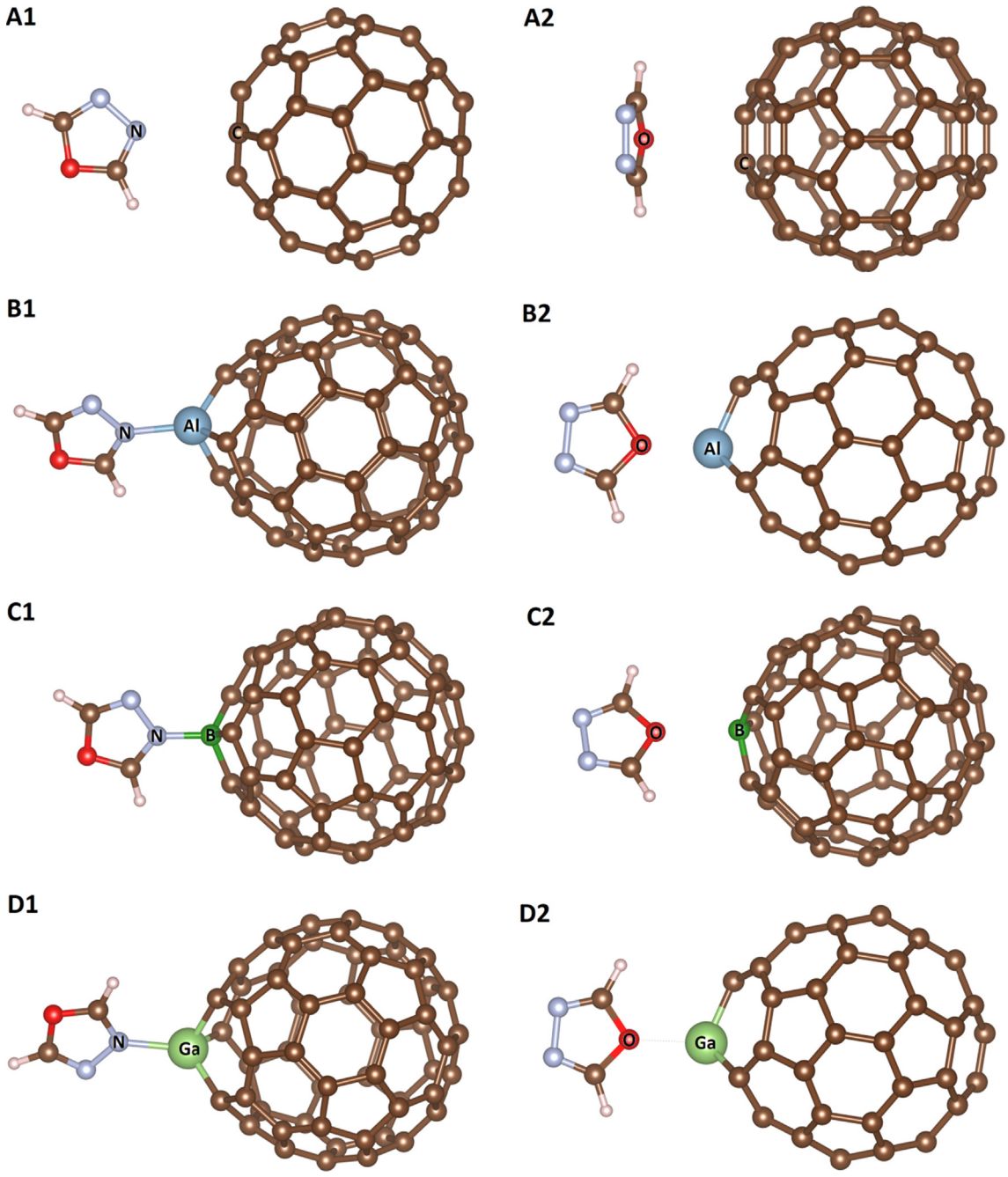

Fig. 1. (Colour online) Relaxed structures of the complexes of the oxadiazole onto the pristine (A1, A2), Al-doped (B1, B2), B-doped (C1, C2), and Ga-doped (D1, D2) C_{60} fullerenes.

2. Computational details

The interaction and the existence of a stable relationship between oxadiazole molecule and pristine, B-, Al-, and Ga-doped C_{60} fullerenes were performed based on DFT calculations using the B3LYP functional and 6-311G(d,p) basis set [44] and the addition of an empirical dispersion term of Grimme's three-parameter [45]. Vibrational frequency are also calculated using Gaussian-09 program package [46] at the same level of theory. Adsorption energies (E_{ads}) for optimized complexes were calculated by following equation:

$$E_{ads} = \left\{E\left(\frac{oxa.}{full.}\right) or E\left(\frac{oxa.}{dopedfull.}\right)\right\} - \{E(full.) or E(dopedfull.)\} - E(oxa.) + E(BSSE) \quad (1)$$

where $E\left(\frac{oxa.}{full.}\right)$ and $E\left(\frac{oxa.}{dopedfull.}\right)$ are the total energies of the oxadiazole molecule adsorbed upon pristine and doped C_{60} fullerenes, respectively. *E(BSSE)* is also known as the basis set superposition error (*BSSE*), which is calculated by the counterpoise method to determine highly accurate adsorption energy [47].

It is well known that the B3LYP functional can underestimate adsorption/binding energies, and some form of dispersion should be included in the DFT exchange-correlation functional to get accurate results. For example, the following recent study on fullerenes has shown dispersion effects to be quite important for fullerenes [48]. The B3LYP functional can also significantly underestimate HOMO/LUMO energies since it only has a 20% fraction of nonlocal exchange, as opposed to a 100% fraction that the exact exchange-correlation functional is known to obey. One way to obtain

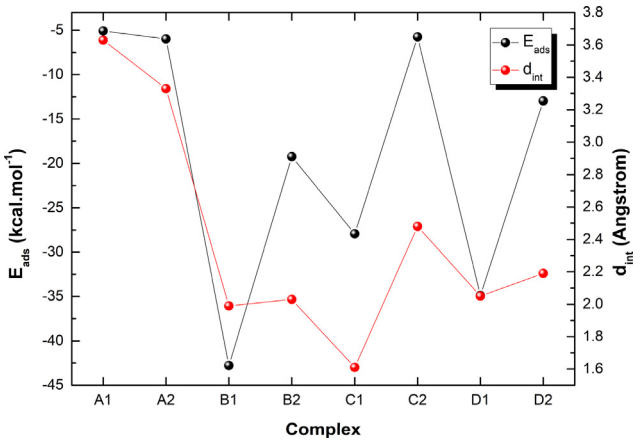

Fig. 2. (Colour online) Adsorption energy (E_{ads}) and interaction distance (d_{int}) of the complexes of the oxadiazole onto the pristine (A1, A2), Al-doped (B1, B2), B-doped (C1, C2), and Ga-doped (D1, D2) C_{60} fullerenes.

accurate HOMO/LUMO energies is to use a range-separated functional, such as those used in the following studies to obtain accurate energies [49,50].

Density of state (DOS) calculations were performed by utilizing GaussSum program [51]. For oxadiazole molecule adsorbed upon pristine and doped C_{60} fullerenes, the quantum molecular descriptors [52] chemical hardness (η), chemical potential (μ), electrophilicity index (ω) and maximum amount of electronic charge index (ΔN_{tot}) were calculated from Koopman's theorem [53], which gives an easy way to identify the ionization potential (I) and electron affinity (A) through the energies of the highest occupied molecular orbital (-E_{HOMO}) and the lowest unoccupied molecular orbital (-E_{LUMO}), using orbital energies as following: $\eta = (I - A)/2$, $\omega = \mu^2/2\eta$ and $\Delta N_{tot} = -\mu/\eta$. Besides, the vertical ionization potential (VIP) and vertical electron affinity (VEA) were calculated using the following expressions: $[VIP = E^{cation} - E^{neutral}]$ and $[VEA = E^{neutral} - E^{anion}]$. Multiwfn program [54] was carried out to obtain Wiberg bond index (WBI) and Fuzzy bond order (FBO), which allow to more understand the relationship between the molecule and surface.

3. Results and discussions

The optimized geometries for interaction between oxadiazole and the pristine or doped C_{60} fullerenes and the two most stable complexes for each configuration (pristine, Al-, B- and Ga-doped C_{60} fullerene) have been presented in Fig. 1. Also, the optimized cartesian coordinates for interactions between oxadiazole and pristine/doped C_{60} fullerenes are given in Tables S1-S8 (as Supporting Information).

Pristine C_{60} fullerene consists of two hexagons and the other shared between a hexagon and pentagon. In this study, the two hexagons and a hexagon and pentagon bond distance of pristine C_{60} fullerene is found as 1.45 and 1.39 Å, which are in good agreement with the experimental data (1.45 and 1.40 Å) of Hedberg et al. [55].

In this study, we initially substituted one of the C atoms with the dopant atom as B, Al and Ga and conjugated it with the functional group of oxadiazole and the obtained complexes were optimized. Compared to Al and Ga atoms, B atom has a smaller diameter than C atom. It is seen that all the dopant atoms caused certain deformations at the point where they were doped in the C_{60} fullerene (see Fig. 1). It is worth noting that deformation becomes more pronounced because the size of Al and Ga atoms are larger than a C atom. However, it is found that there is no imaginary frequency that implies the transition state at a saddle-point on the potential energy surface.

Depending on the interaction between oxadiazole and pristine/doped C_{60} fullerene, there are eight stable complexes called A1, A2, B1, B2, C1, C2, D1 and D2. As shown in Fig. 1, two stable oxadiazole/fullerene complexes were found in which the

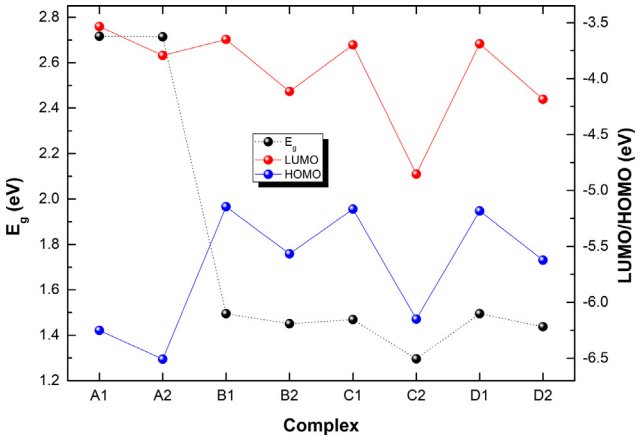

Fig. 3. (Colour online) The HOMO-LUMO energy gap (E_g) of the complexes of the oxadiazole onto the pristine (A1, A2), Al-doped (B1, B2), B-doped (C1, C2), and Ga-doped (D1, D2) C_{60} fullerenes.

Table 1
The structural and energetic properties of pristine (A) and Al-doped (B), B-doped (C) and Ga-doped (D) C60 fullerene as well as interaction between oxadiazole and the pristine (A1, A2), Al-doped (B1, B2), B-doped (C1, C2) and Ga-doped (D1, D2) C_{60} fullerenes and the two stable complexes (d_{int} is Å, E_{ads} is kcal mol^{-1}, and the others are in eV).

	A	A1	A2	B	B1	B2	C	C1	C2	D	D1	D2
E_{ads}	–	−5.07	−5.98	–	−42.78	−19.24	–	−27.93	−5.75	–	−34.90	−12.97
d_{int}	–	3.63	3.33	–	1.99	2.03	–	1.61	2.48	–	2.05	2.19
HOMO	−6.40	−6.25	−6.51	−5.75	−5.14	−5.57	−6.06	−5.17	−6.15	−5.81	−5.18	−5.62
LUMO	−3.66	−3.53	−3.79	−5.37	−3.65	−4.11	−4.77	−3.70	−4.85	−4.45	−3.69	−4.19
E_g	2.74	2.72	2.71	1.38	1.50	1.45	1.29	1.47	1.30	1.36	1.50	1.44
VIP	7.61	7.44	7.62	6.89	6.26	6.66	7.23	6.28	7.20	6.95	6.29	6.76
VEA	2.45	2.33	2.51	3.24	2.56	2.99	3.59	2.60	3.60	3.32	2.60	3.10
η	1.37	1.36	1.36	0.69	0.75	0.73	0.65	0.73	0.65	0.68	0.75	0.72
μ	−5.03	−4.89	−5.15	−5.06	−4.40	−4.44	−5.41	−4.43	−5.10	−5.13	−4.44	−4.51
ω	9.23	8.81	9.77	18.55	12.93	13.38	22.66	13.37	19.70	19.40	13.16	13.93
ΔN_{tot}	3.67	3.60	3.80	7.34	5.88	6.03	8.37	6.03	7.73	7.57	5.93	6.18
WBI	–	–	–	–	0.63	0.42	–	0.86	0.13	–	0.70	0.48
FBO	–	–	–	–	0.77	0.48	–	0.76	0.14	–	0.82	0.31
f_{min}	–	13.75	12.21	–	23.41	21.44	–	40.02	12.32	–	23.03	18.97

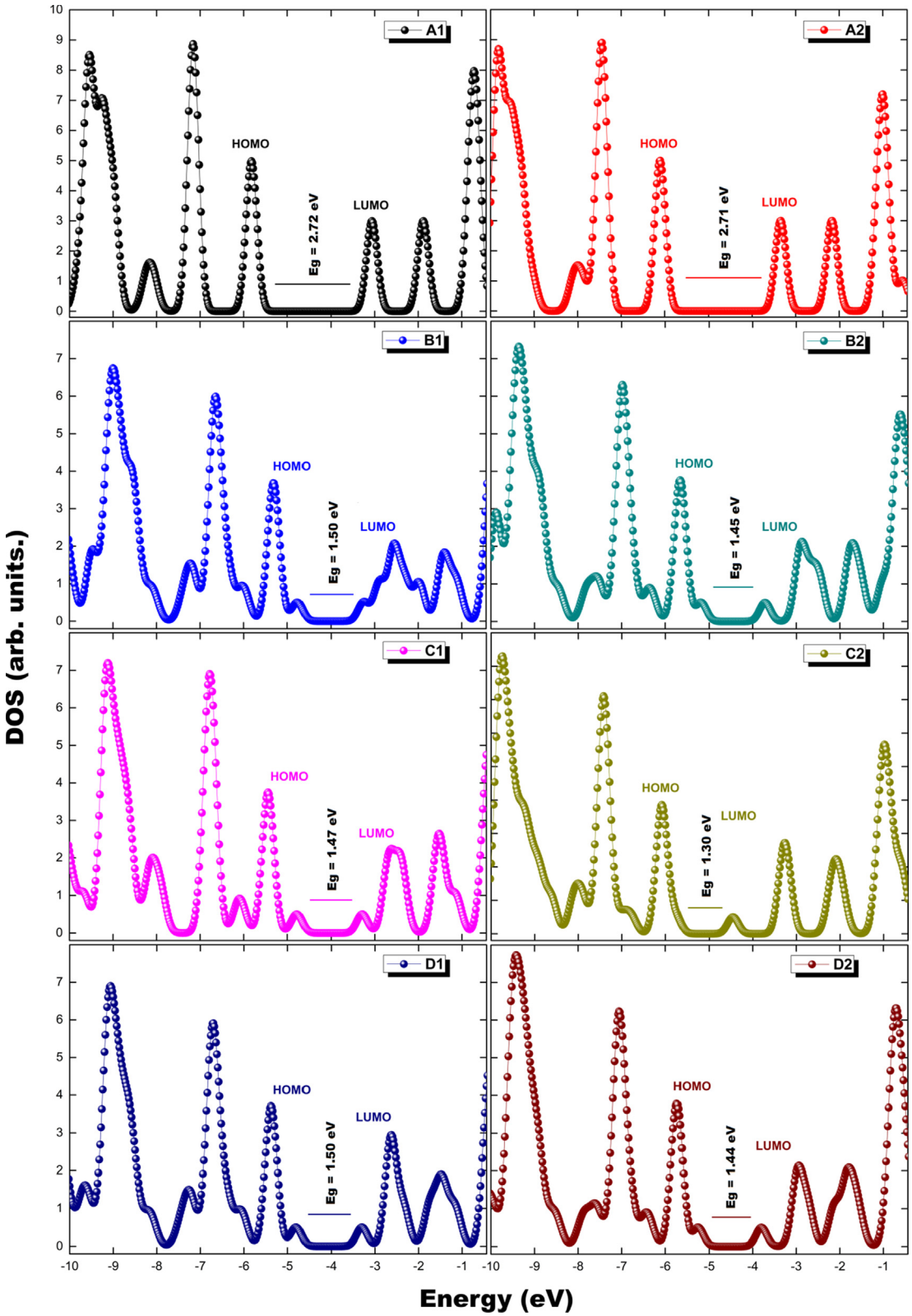

Fig. 4. (Colour online) Density of states (DOS) of the complexes of the oxadiazole onto the pristine (A1, A2), Al-doped (B1, B2), B-doped (C1, C2), and Ga-doped (D1, D2) C_{60} fullerenes.

oxadiazole attaches to the C/Al/B/Ga atoms from its nitrogen (complex N-C/Al/B/Ga; A1, B1, C1 and D1) or oxygen (complex O-C/Al/B/Ga; A2, B2, C2 and D2) atom.

Adsorption energy (E_{ads}) and interaction distance (d_{int}) of complexes are found to be −5.07 kcal.mol^{-1} and 3.63 Å (for A1 complex) and −5.98 kcal.mol^{-1} and 3.33 Å (for A2 complex),

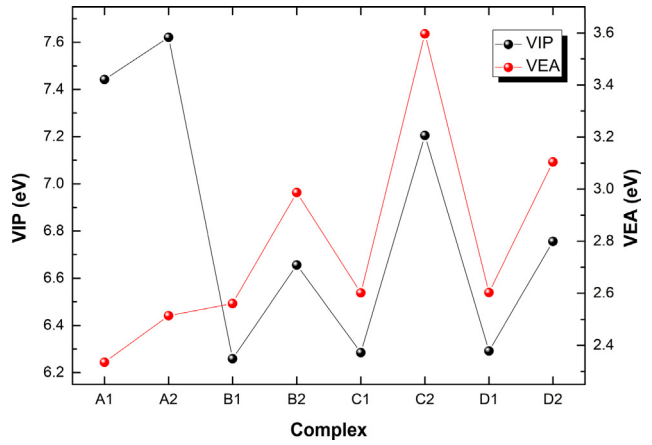

Fig. 5. (Colour online) Vertical ionization potential (VIP) and vertical electron affinity (VEA) of the complexes of the oxadiazole onto the pristine (A1, A2), Al-doped (B1, B2), B-doped (C1, C2), and Ga-doped (D1, D2) C_{60} fullerenes.

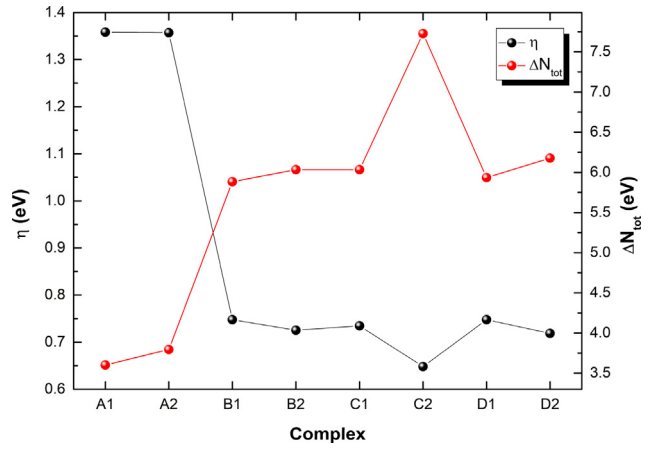

Fig. 6. (Colour online) Chemical hardness (η) and maximum amount electronic charge index (ΔN_{tot}) of the complexes of the oxadiazole onto the pristine (A1, A2), Al-doped (B1, B2), B-doped (C1, C2), and Ga-doped (D1, D2) C_{60} fullerenes.

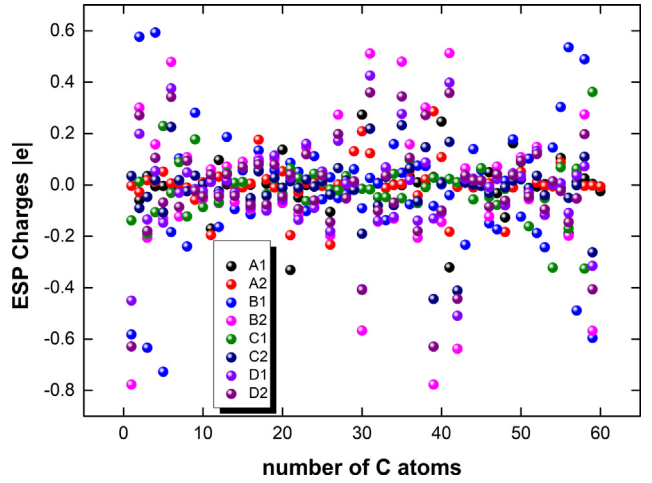

Fig. 7. (Colour online) The electrostatic potential (ESP) charges of the complexes of the oxadiazole onto the pristine (A1, A2), Al-doped (B1, B2), B-doped (C1, C2), and Ga-doped (D1, D2) C_{60} fullerenes.

indicating weak interaction, which probably is due to the existence of physisorption between oxadiazole and C_{60} fullerene. Furthermore, it clearly seen that the E_{ads} increases significantly after dopants are introduced to C_{60} fullerene (see Fig. 2). In two stable complexes for Al-doped configuration, oxadiazole molecule is adsorbed from its Al --- N (B1 complex) and Al --- O (B2 complex) heads on Al-doped C_{60} fullerene; the distance between two structure was calculated to be 1.99 and 2.03 Å, and E_{ads} were about −42.78 and −19.24 kcal.mol^{-1} (see Table 1). For B- and Ga-doped configurations, similarly, oxadiazole is adsorbed from its B/Ga --- N (C1/D1 complexes) and B/Ga --- O (C2/D2 complexes) heads on doped C_{60} fullerene. Results indicate that mainly the B, Al, and Ga atoms in doped C_{60} fullerenes than C atoms more likely to have an interaction with the N and O atoms of oxadiazole molecule (see Fig. 1). In addition, E_{ads} values are about −19.24, −5.75 and −12.97 kcal.mol^{-1} for B2, C2 and D2 complexes, indicating that there are relatively weak interactions between oxygen and dopant atoms. Therefore, the oxadiazole do not adsorb efficiently on the surface of the doped C_{60} fullerene through these configurations. A comparison of the calculated E_{ads} and d_{int} for the adsorption of oxadiazole on the Al-, B- and Ga-doped C_{60} fullerene shows that the bind of N on the doped C_{60} fullerene (B1, C1 and D1 complexes) is much stronger than that of O.

The HOMO-LUMO energy gap (E_g) values for interaction between oxadiazole molecule and Al-, B- and Ga-doped C_{60} fullerenes are much lower than that of pristine C_{60} fullerene (see Fig. 3), that is, an increase in energy gap energy causes a reduction in the electrical conductivity after dopants are introduced to C_{60} fullerene. It is concluded that B-, Al- and Ga-doped C_{60} fullerenes can detect the occurrence of oxadiazole molecule better than pristine C_{60}. As seen in Table 1, the E_g of C_{60} fullerene (A) is found to be 2.74 eV, that of the pristine C_{60} fullerene configuration is calculated in the range of 2.72 (A1 complex) to 2.71 eV (A2 complex) after oxadiazole interaction. These results display that the E_g remains invariant and no distinct change of energy gap energy is observed by the oxadiazole adsorption for these configurations. After oxadiazole adsorption, the E_g of the Al-, B- and Ga-doped configurations increases from 1.38 (B configuration) to 1.50 (B1 complex) and 1.45 eV (B2 complex), from 1.29 (C configuration) to 1.47 (C1 complex) and 1.30 eV (C2 complex) and from 1.36 (D configuration) to 1.50 (D1 complex) and 1.44 eV (D2 complex), respectively (see Table 1). These results indicate that adsorption decreases the electrical conductivity of the configurations. Fig. 4 shows the density of states (DOS) in the energy range −10 to −0.5 eV. After oxadiazole adsorption, a big shift near the HOMO levels compared to that of the pristine C_{60} fullerene was seen, whereas LUMO levels do not shift to higher energy. Our results clarify after oxadiazole adsorption the energy gaps for interaction between oxadiazole and doped C_{60} fullerene has noteworthy decreases. Therefore, it is concluded that Al-doped C_{60} fullerene can be a better candidate for the carrier of oxadiazole.

After oxadiazole adsorption the *VIP* of the Al-, B- and Ga-doped configurations decreases from 6.89 (B configuration) to 6.26 (B1 complex) and 6.66 eV (B2 complex), from 7.23 (C configuration) to 6.28 (C1 complex) and 7.20 eV and from 6.95 (D configuration) to 6.29 (D1 complex) and 6.76 eV (D2 complex), respectively (see Table 1). Similarly, the *VEA* of the Al-, B- and Ga-doped configurations decreases generally when dopants are introduced to C_{60} fullerene. All these results clearly show that dopant atoms decrease generally the ionization potential and electron affinity of the configurations (see Fig. 5).

After oxadiazole adsorption, the E_g of the Al-, B- and Ga-doped configurations increases from 0.69 (B configuration) to 0.75 (B1 complex) and 0.73 eV (B2 complex), from 0.65 (C configuration) to 0.73 eV (C1 complex) and from 0.68 (D configuration) to 0.75 (D1 complex) and 0.72 eV (D2 complex), respectively (see Table 1). Besides, the N_{tot} of Al-, B- and Ga-doped configurations decreases generally when dopants are introduced to C_{60} fullerene. This can

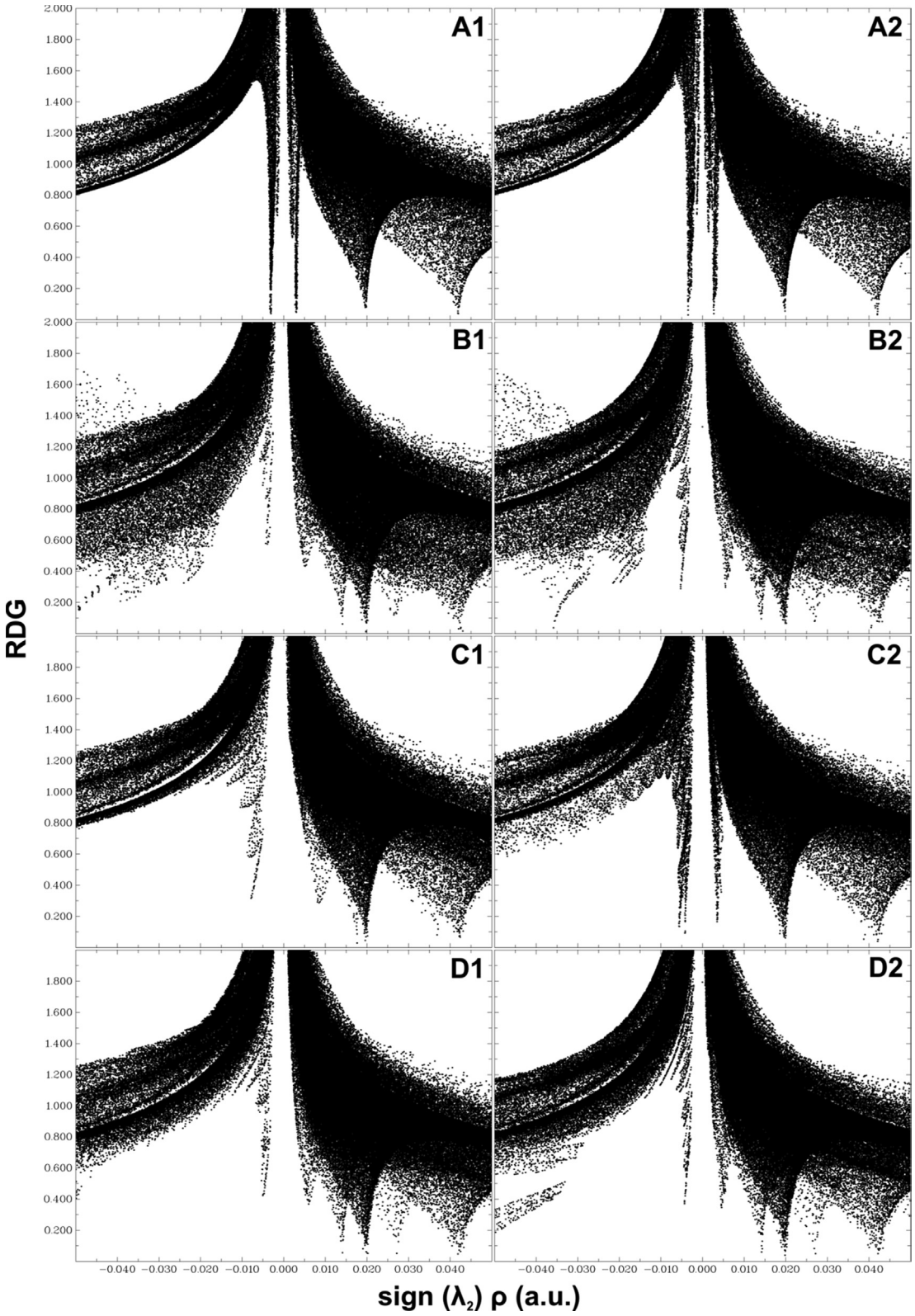

Fig. 8. The reduced density gradient (RDG) scatter plots of the complexes of the oxadiazole onto the pristine (A1, A2), Al-doped (B1, B2), B-doped (C1, C2), and Ga-doped (D1, D2) C_{60} fullerenes.

be due to the relatively more strongly nucleophilic property, relatively higher hybridization levels, and out of plan character of the dopant atoms compared to C. This infers that the reactivity of oxadiazole molecule is relatively high in these configurations owing to the high η and low ω and ΔN_{tot} that leads to decreases significantly the chemical reactivity (see Fig. 6). A comparison of the calculated electronic parameters for the adsorption of oxadiazole on the Al-, B- and Ga-doped C_{60} fullerene indicate that the bind of N on the

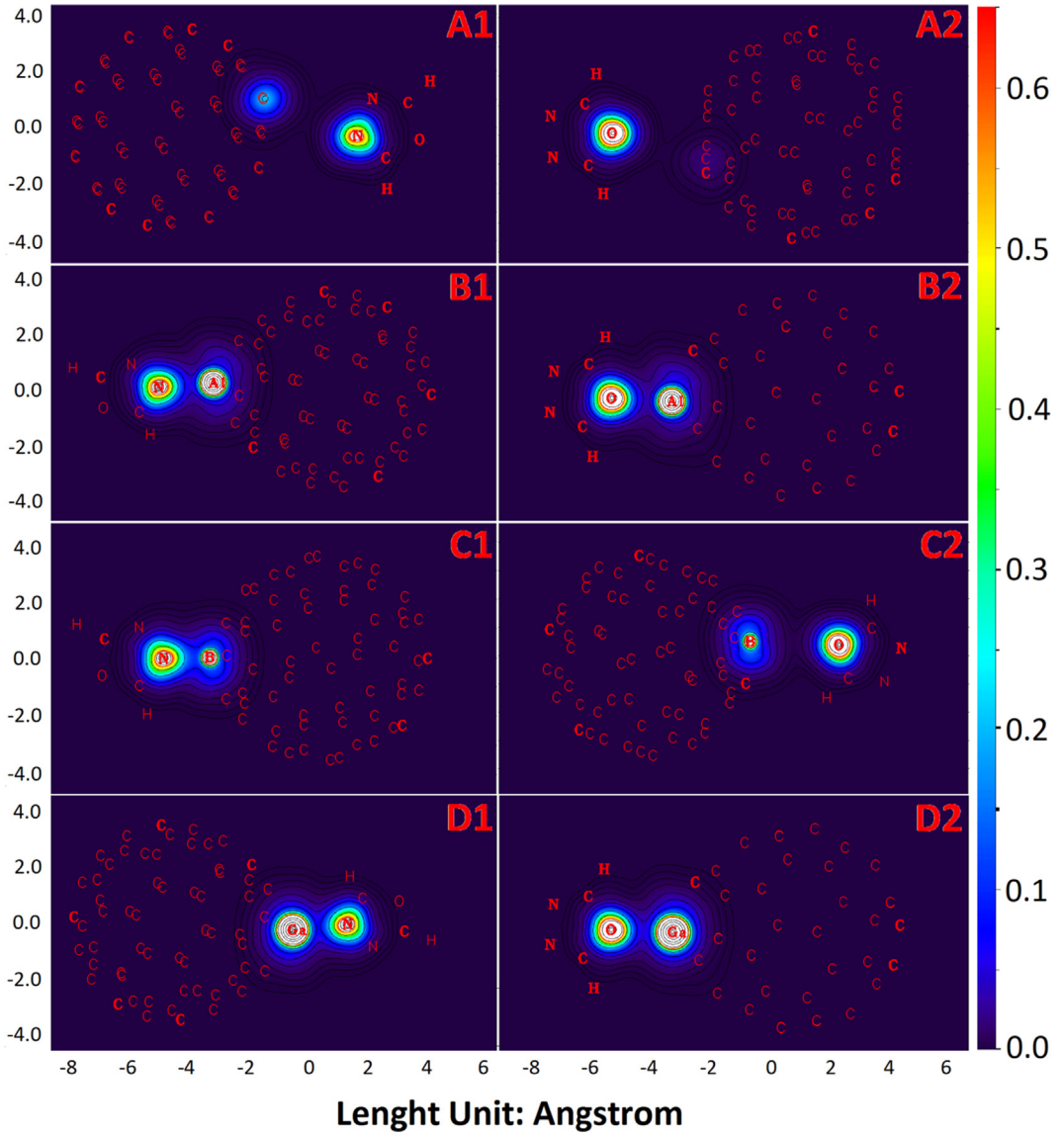

Fig. 9. (Colour online) Contour maps of electron densities of the complexes of the oxadiazole onto the pristine/doped C_{60} fullerenes.

doped C_{60} fullerene (B1, C1 and D1 complexes) is lower in reactivity than that of O.

Comparing to the pristine C_{60} fullerene after the adsorption, the η of doped C_{60} fullerene is decreased significantly and thus this decrease gives rise to low resistance to change in electronic configuration that leads to preferential adsorption on the doped C_{60} fullerene. In addition, it was found that oxadiazole is physically absorbed at the surface of Al-, B- and Ga-doped C_{60} fullerenes and induces a redistribution of electron density with an observable increase in electrostatic potential (ESP) charges on carbon atoms (see in Fig. 7). We note that the electrostatic potential of the Al atom is relatively larger compared to the C or other dopant atoms which makes it a more electrophilic site for N or O atom of oxadiazole.

The active sites for B-, Al- and Ga-doped C_{60} fullerenes according to computed WBI and FBO analyses were considered boron, aluminum, and gallium atoms, respectively. Table 1 shows the bond of the N and O atoms in oxadiazole oriented to the Al/B/Ga atom in doped C_{60} fullerenes. WBI and FBO reveal that doped fullerenes show a strong interaction with the oxadiazole. Comparing to the bond indexes and bond orders of the oxadiazole and doped C_{60} fullerenes after the adsorption, dopant atoms tend to prefer interacting with N atoms due to their higher WBI and FBO values. In addition, the WBI and FBO analyses agree with the adsorption energies and interaction distances shown in Table 1.

The RDG analysis was performed to understand the strength of interactions between pristine/doped C_{60} fullerene and oxadiazole (see Fig. 8). In these plots, the interaction between oxadiazole and Al-doped C_{60} fullerene can be in a strong interaction region in B1 and B2 complexes, whereas the interactions between the oxadiazole and B- and Ga-doped C_{60} fullerene are weak. Furthermore, the repulsion interactions between oxadiazole and Al- and Ga-doped C_{60} fullerene are slightly greater than that in the B-doped C_{60} fullerene.

Fig. 9 shows the contour maps of electron density for interactions between the N/O atoms and dopant atoms based on adsorption states of oxadiazole molecule onto the pristine/doped C_{60} fullerenes. It is clear that the N and O atoms in oxadiazole are oriented to the Al/B/Ga atom in doped C_{60} fullerenes, and thus the electron density is transferred from one of N atom or O atom to dopant atoms. We note that the electron density of the dopant atoms is significantly larger compared to the carbon atom which

makes it a more electrophilic site for N or O atom of oxadiazole. We also notice that the electron density of N-binding interactions with dopant atoms is bigger than that of O-binding interactions (see Fig. 9).

4. Conclusions

The adsorption behavior of oxadiazole molecule on pristine, B-, Al- and Ga-doped C_{60} fullerenes have been predicted using density functional theory (DFT). It is found that the dopant atoms improve the chemical reactivity of C_{60} but reduce the electronic sensitivity toward the oxadiazole. Furthermore, the adsorption energy and energy gap for the interactions between the oxadiazole and the B-, Al- and Ga-doped C_{60} increase in comparison with the pristine C_{60}. The highest adsorption capacity was also found when using Al dopant with releasing energy about of -42.78 kcal.mol^{-1}. WBI and FBO analyses show a possible bonding interaction between the dopants in fullerenes and the N or O atom in the oxadiazole molecule, possibly due to a significant change in charge carrier mobility. This result can be a sign of the existence of a stable relationship between the N atom in the oxadiazole and Al atom in the doped fullerene. It could be concluded that the oxadiazole can be better adsorbed on Al/B/Ga sites of doped C_{60} fullerene with forming the Al/B/Ga–N bond. The results of electron density also support this possibility. Therefore, we note that Al-doped C_{60} fullerenes would be preferable as a candidate for the adsorption of the oxadiazole.

CRediT authorship contribution statement

İskender Muz: Investigation, Methodology, Conceptualization, Visualization, Writing - original draft, Writing - review & editing, Data curation, Software. **Mustafa Kurban:** Supervision, Investigation, Writing - original draft, Writing - review & editing.

Declaration of Competing Interest

The authors declare that they have no known competing financial interests or personal relationships that could have appeared to influence the work reported in this paper.

Acknowledgments

The numerical calculations reported were partially performed at TUBITAK ULAKBIM, High Performance and Grid Computing Centre (TRUBA resources), Turkey.

Appendix A. Supplementary data

Supplementary data to this article can be found online at https://doi.org/10.1016/j.molliq.2021.116181.

References

[1] A. Ben Saïd, A. Romdhane, N. Elie, D. Touboul, H. Ben Jannet, J. Bouajila, Design, synthesis of novel pyranotriazolopyrimidines and evaluation of their anti-soybean lipoxygenase, anti-xanthine oxidase, and cytotoxic activities, J. Enzyme Inhib. Med. Chem. 31 (2016) 1277–1285, https://doi.org/10.3109/14756366.2015.1118684.
[2] N.P. Rai, V.K. Narayanaswamy, T. Govender, B.K. Manuprasad, S. Shashikanth, P.N. Arunachalam, Design, synthesis, characterization, and antibacterial activity of 5-chloro-2-[(3-substitutedphenyl-1,2,4-oxadiazol-5-yl)-methoxy]-phenyl -(phenyl)-methanones, Eur. J. Med. Chem. 45 (2010) 2677–2682, https://doi.org/10.1016/j.ejmech.2010.02.021.
[3] S. Ningaiah, U.K. Bhadraiah, S. Keshavamurthy, C. Javarasetty, Novel pyrazoline amidoxime and their 1,2,4-oxadiazole analogues: Synthesis and pharmacological screening, Bioorg. Med. Chem. Lett. 23 (2013) 4532–4539, https://doi.org/10.1016/j.bmcl.2013.06.042.
[4] M. Farooqui, R. Bora, C.R. Patil, Synthesis, analgesic and anti-inflammatory activities of novel 3-(4-acetamido-benzyl)-5-substituted-1,2,4-oxadiazoles, Eur. J. Med. Chem. 44 (2009) 794–799, https://doi.org/10.1016/j.ejmech.2008.05.022.
[5] R. Bhutani, D.P. Pathak, G. Kapoor, A. Husain, M.A. Iqbal, Novel hybrids of benzothiazole-1,3,4-oxadiazole-4-thiazolidinone: Synthesis, in silico ADME study, molecular docking and in vivo anti-diabetic assessment, Bioorg. Chem. 83 (2019) 6–19, https://doi.org/10.1016/j.bioorg.2018.10.025.
[6] L.H. Al-Wahaibi, N. Santhosh Kumar, A.A. El-Emam, N.S. Venkataramanan, H.A. Ghabbour, A.M.S. Al-Tamimi, J. Percino, S. Thamotharan, Investigation of potential anti-malarial lead candidate 2-(4-fluorobenzylthio)-5-(5-bromothiophen-2-yl)-1,3,4-oxadiazole: Insights from crystal structure, DFT, QTAIM and hybrid QM/MM binding energy analysis, J. Mol. Struct. 1175 (2019) 230–240, https://doi.org/10.1016/j.molstruc.2018.07.102.
[7] H. Khalilullah, S. Khan, M.S. Nomani, B. Ahmed, Synthesis, characterization and antimicrobial activity of benzodioxane ring containing 1,3,4-oxadiazole derivatives, Arab. J. Chem. 9 (2016) S1029–S1035, https://doi.org/10.1016/j.arabjc.2011.11.009.
[8] J. Sławiński, K. Szafrański, A. Pogorzelska, B. Żołnowska, A. Kawiak, K. Macur, M. Belka, T. Bączek, Novel 2-benzylthio-5-(1,3,4-oxadiazol-2-yl) benzenesulfonamides with anticancer activity: synthesis, QSAR study, and metabolic stability, Eur. J. Med. Chem. 132 (2017) 236–248, https://doi.org/10.1016/j.ejmech.2017.03.039.
[9] A. Husain, A. Ahmad, M.M. Alam, M. Ajmal, P. Ahuja, Fenbufen based 3-[5-(substituted aryl)-1,3,4-oxadiazol-2-yl]-1-(biphenyl-4-yl)propan-1-ones as safer antiinflammatory and analgesic agents, Eur. J. Med. Chem. 44 (2009) 3798–3804, https://doi.org/10.1016/j.ejmech.2009.04.009.
[10] M. Amir, S.A. Javed, H. Kumar, Synthesis and biological evaluation of some 4-(1H-indol-3-yl)-6-phenyl-1,2, 3,4-tetrahydropyrimidin-2-ones/thiones as potent anti-inflammatory agents, Acta Pharm. 58 (2008) 467–477, https://doi.org/10.2478/v10007-008-0028-x.
[11] I. Muz, M. Kurban, M. Dalkilic, DFT and TD-DFT studies of new pentacene-based organic molecules as a donor material for bulk-heterojunction solar cells, J. Comput. Electron. 19 (2020) 895–904, https://doi.org/10.1007/s10825-020-01493-7.
[12] N.M.R. Peres, The electronic properties of graphene and its bilayer, Vacuum 83 (2009) 1248–1252, https://doi.org/10.1016/j.vacuum.2009.03.018.
[13] E. Llobet, Gas sensors using carbon nanomaterials: a review, Sens. Actuators, B Chem. 179 (2013) 32–45, https://doi.org/10.1016/j.snb.2012.11.014.
[14] L. Dai, D.W. Chang, J.-B. Baek, W. Lu, Carbon nanomaterials for advanced energy conversion and storage, Small 8 (2012) 1130–1166, https://doi.org/10.1002/smll.201101594.
[15] Y.H. Park, H.H. Rho, N.G. Park, Y.S. Kim, Theoretical investigation of tetra-substituted pyrenes for organic light emitting diodes, Curr. Appl. Phys. 6 (2006) 691–694, https://doi.org/10.1016/j.cap.2005.04.021.
[16] M. Noei, DFT study on the sensitivity of open edge graphene toward CO2 gas, Vacuum 131 (2016) 194–200, https://doi.org/10.1016/j.vacuum.2016.06.018.
[17] M. Najafi, Density functional study of cyanogen (C2N2) sensing using OH functionalized fullerene (C60) and germanium-fullerene (Ge60), Vacuum 134 (2016) 88–91, https://doi.org/10.1016/j.vacuum.2016.10.001.
[18] M. Reza Jalali Sarvestani, R. Ahmadi, B. Farhang Rik, Procarbazine adsorption on the surface of single walled carbon nanotube: DFT studies, Chem. Rev. Lett. 3 (2020) 175–179.
[19] H.G. Rauf, E.A. Mahmood, S. Majedi, M. Sofi, Adsorption behavior of the Al-and Ga-doped B12N12 nanocages on COn (n=1, 2) and HnX (n=2, 3 and X=O, N): a comparative study, Chem. Rev. Lett. 2 (2019) 140–150.
[20] R. Rostamoghli, M. Vakili, A. Banaei, E. Pourbashir, K. Jalalierad, Applying the B12N12 nanoparticle as the CO, CO2, H2O and NH3 sensor, Chem Rev Lett. 1 (2018) 31–36, https://doi.org/10.22034/CRL.2018.85214.
[21] E. Babanezhad, A. Beheshti, The possibility of selective sensing of the straight-chain alcohols (including methanol to n-pentanol) by using the C20 fullerene and C18NB nano cage, Chem. Rev. Lett. 1 (2018) 82–88.
[22] S.A. Siadati, S. Rezazadeh, Switching behavior of an actuator containing germanium, silicon-decorated and normal C20 fullerene, Chem. Rev. Lett. 1 (2018) 77–81.
[23] J. Li, Y. Lu, Q. Ye, M. Cinke, J. Han, M. Meyyappan, Carbon nanotube sensors for gas and organic vapor detection, Nano Lett. 3 (2003) 929–933, https://doi.org/10.1021/nl034220x.
[24] Q. Shi, F. Peng, S. Liao, H. Wang, H. Yu, Z. Liu, B. Zhang, D. Su, Sulfur and nitrogen co-doped carbon nanotubes for enhancing electrochemical oxygen reduction activity in acidic and alkaline media, J. Mater. Chem. A. 1 (2013) 14853–14857, https://doi.org/10.1039/c3ta12647a.
[25] M. Kurban, İ. Muz, Theoretical investigation of the adsorption behaviors of fluorouracil as an anticancer drug on pristine and B-, Al-, Ga-doped C36 nanotube, J. Mol. Liq. 309 (2020), https://doi.org/10.1016/j.molliq.2020.113209 113209.
[26] L. Li, B. Yu, T. You, Nitrogen and sulfur co-doped carbon dots for highly selective and sensitive detection of Hg (II) ions, Biosens. Bioelectron. 74 (2015) 263–269, https://doi.org/10.1016/j.bios.2015.06.050.
[27] J.N. Gavgani, A. Hasani, M. Nouri, M. Mahyari, A. Salehi, Highly sensitive and flexible ammonia sensor based on S and N co-doped graphene quantum dots/polyaniline hybrid at room temperature, Sens. Actuators, B Chem. 229 (2016) 239–248, https://doi.org/10.1016/j.snb.2016.01.086.
[28] M.D. Esrafili, BN co-doped graphene monolayers as promising metal-free catalysts for N2O reduction: a DFT study, Chem. Phys. Lett. 705 (2018) 44–49, https://doi.org/10.1016/j.cplett.2018.05.054.

[29] İ. Muz, F. Göktaş, M. Kurban, 3d-transition metals (Cu, Fe, Mn, Ni, V and Zn)-doped pentacene π-conjugated organic molecule for photovoltaic applications: DFT and TD-DFT calculations, Theor. Chem. Acc. 139 (2020) 1–8, https://doi.org/10.1007/s00214-020-2544-9.
[30] İ. Muz, M. Kurban, A comprehensive study on electronic structure and optical properties of carbon nanotubes with doped B, Al, Ga, Si, Ge, N, P and As and different diameters, J. Alloys Compd. 802 (2019) 25–35, https://doi.org/10.1016/j.jallcom.2019.06.210.
[31] M.D. Ganji, H. Yazdani, Interaction between B-doped C_{60} fullerene and glycine amino acid from first-principles simulation, Chin. Phys. Lett. 27 (2010), https://doi.org/10.1088/0256-307X/27/4/043102 043102.
[32] M.K. Hazrati, N.L. Hadipour, Adsorption behavior of 5-fluorouracil on pristine, B-, Si-, and Al-doped C60 fullerenes: A first-principles study, Phys. Lett. Sect. A Gen. At. Solid State Phys. 380 (2016) 937–941, https://doi.org/10.1016/j.physleta.2016.01.020.
[33] M. Moradi, M. Nouraliei, R. Moradi, Theoretical study on the phenylpropanolamine drug interaction with the pristine, Si and Al doped [60] fullerenes, Phys. E Low-Dimensional Syst. Nanostruct. 87 (2017) 186–191, https://doi.org/10.1016/j.physe.2016.11.027.
[34] Y. Wang, M. Jiao, W. Song, Z. Wu, Doped fullerene as a metal-free electrocatalyst for oxygen reduction reaction: a first-principles study, Carbon N. Y. 114 (2017) 393–401, https://doi.org/10.1016/j.carbon.2016.12.028.
[35] M.D. Esrafili, N. Mohammadirad, A first-principles study on the adsorption behaviour of methanol and ethanol over C_{59} B heterofullerene, Mol. Phys. 115 (2017) 1633–1641, https://doi.org/10.1080/00268976.2017.1311423.
[36] F. Hassani, H. Tavakol, A DFT AIM and NBO study of adsorption and chemical sensing of iodine by S-doped fullerenes, Sens. Actuators, B Chem. 196 (2014) 624–630, https://doi.org/10.1016/j.snb.2014.02.051.
[37] Q.Z. Li, J.J. Zheng, J.S. Dang, X. Zhao, Boosting activation of oxygen molecules on C60 fullerene by boron doping, ChemPhysChem. 16 (2015) 390–395, https://doi.org/10.1002/cphc.201402620.
[38] F. Gao, G.L. Zhao, S. Yang, J.J. Spivey, Nitrogen-doped fullerene as a potential catalyst for hydrogen fuel cells, J. Am. Chem. Soc. 135 (2013) 3315–3318, https://doi.org/10.1021/ja309042m.
[39] Y. Hashikawa, M. Murata, A. Wakamiya, Y. Murata, Synthesis and properties of endohedral Aza[60]fullerenes: H2O@C59N and H2@C59N as their dimers and monomers, J. Am. Chem. Soc. 138 (2016) 4096–4104, https://doi.org/10.1021/jacs.5b12795.
[40] R. Eigler, F.W. Heinemann, A. Hirsch, Hydro-aza-(C_{59} N)fullerenes: formation mechanism and hydrogen substitution, Chem. - A Eur. J. 22 (2016) 13575–13581, https://doi.org/10.1002/chem.201505115.
[41] Y. García-Rodeja, M. Sola, I. Fernandez, Predicting and understanding the reactivity of aza[60]fullerenes, J. Org. Chem. 82 (2017) 754–758, https://doi.org/10.1021/acs.joc.6b02424.
[42] İ. Muz, M. Kurban, The electronic structure, transport and structural properties of nitrogen-decorated graphdiyne nanomaterials, J. Alloys Compd. 842 (2020), https://doi.org/10.1016/j.jallcom.2020.155983 155983.
[43] C.D. Mohan, N.C. Anilkumar, S. Rangappa, M.K. Shanmugam, S. Mishra, A. Chinnathambi, S.A. Alharbi, A. Bhattacharjee, G. Sethi, A.P. Kumar, K.S. Rangappa Basappa, Novel 1,3,4-oxadiazole induces anticancer activity by targeting NF-κB in hepatocellular carcinoma cells, Front. Oncol. 8 (2018) 42, https://doi.org/10.3389/fonc.2018.00042.
[44] A.D. Becke, A new mixing of hatree-fock and local density functional theories, J. Chem. Phys. 98 (1993) 1372–1377, https://doi.org/10.1063/1.464304.
[45] S. Grimme, S. Ehrlich, L. Goerigk, Effect of the damping function in dispersion corrected density functional theory, J. Comput. Chem. 32 (2011) 1456–1465, https://doi.org/10.1002/jcc.21759.
[46] M.J. Frisch, G.W. Trucks, H.B. Schlegel, G.E. Scuseria, M.A. Robb, J.R. Cheeseman, G. Scalmani, V. Barone, B. Mennucci, G.A. Petersson, H. Nakatsuji, M. Caricato, X. Li, H.P. Hratchian, A.F. Izmaylov, J. Bloino, G. Zheng, J.L. Sonnenberg, M. Hada, M. Ehara, K. Toyota, R. Fukuda, J. Hasegawa, M. Ishida, T. Nakajima, Y. Honda, O. Kitao, H. Nakai, T. Vreven, J.A. Montgomery, J.E. Peralta, F. Ogliaro, M. Bearpark, J.J. Heyd, E. Brothers, K.N. Kudin, V.N. Staroverov, R. Kobayashi, J. Normand, K. Raghavachari, A. Rendell, J.C. Burant, S.S. Iyengar, J. Tomasi, M. Cossi, N. Rega, J.M. Millam, M. Klene, J.E. Knox, J.B. Cross, V. Bakken, C. Adamo, J. Jaramillo, R. Gomperts, R.E. Stratmann, O. Yazyev, A.J. Austin, R. Cammi, C. Pomelli, J.W. Ochterski, R.L. Martin, K. Morokuma, V.G. Zakrzewski, G.A. Voth, P. Salvador, J.J. Dannenberg, S. Dapprich, A.D. Daniels, Farkas, J.B. Foresman, J. V Ortiz, J. Cioslowski, D.J. Fox, Gaussian 09, Revision E.01, Gaussian Inc., Wallingford CT. (2009).
[47] S.F. Boys, F. Bernardi, The calculation of small molecular interactions by the differences of separate total energies. Some procedures with reduced errors, Mol. Phys. 19 (1970) 553–566, https://doi.org/10.1080/00268977000101561.
[48] B.M. Wong, Noncovalent interactions in supramolecular complexes: a study on corannulene and the double concave buckycatcher, J. Comput. Chem. 30 (2009) 51–56, https://doi.org/10.1002/jcc.21022.
[49] B.M. Wong, T.H. Hsieh, Optoelectronic and excitonic properties of oligoacenes: substantial improvements from range-separated time-dependent density functional theory, J. Chem. Theory Comput. 6 (2010) 3704–3712, https://doi.org/10.1021/ct100529s.
[50] M.E. Foster, B.M. Wong, Nonempirically tuned range-separated DFT accurately predicts both fundamental and excitation gaps in DNA and RNA nucleobases, J. Chem. Theory Comput. 8 (2012) 2682–2687, https://doi.org/10.1021/ct300420f.
[51] N.M. O'Boyle, A.L. Tenderholt, K.M. Langner, cclib: a library for package-independent computational chemistry algorithms, J. Comput. Chem. 29 (2008) 839–845, https://doi.org/10.1002/jcc.20823.
[52] R.G. Parr, R.G. Pearson, Absolute hardness - Companion parameter to absolute electronegativity, J. Am. Chem. Soc. 105 (1983) 7512–7516, https://doi.org/10.1021/ja00364a005.
[53] T. Koopmans, Über die Zuordnung von Wellenfunktionen und Eigenwerten zu den Einzelnen Elektronen Eines Atoms, Physica 1 (1934) 104–113, https://doi.org/10.1016/S0031-8914(34)90011-2.
[54] T. Lu, F. Chen, Multiwfn: a multifunctional wavefunction analyzer, J. Comput. Chem. 33 (2012) 580–592, https://doi.org/10.1002/jcc.22885.
[55] K. Hedberg, L. Hedberg, D.S. Bethune, C.A. Brown, H.C. Dorn, R.D. Johnson, M. De Vries, Bond lengths in free molecules of buckminsterfullerene, C60, from gas-phase electron diffraction, Science (80-.) 254 (1991) 410–412, https://doi.org/10.1126/science.254.5030.410.